Supplementary Information: The emergence of bulk structure in clusters via isotropic multi-well pair potentials

Jennifer E. Doyle,[1,2] Maya M. Martirossyan,[3,2,4] Julia Dshemuchadse,[3,5] and Erin G. Teich[1,6]
[1)] *Department of Physics and Astronomy, Wellesley College, Wellesley, MA*
[2)] *These authors contributed equally to this work*
[3)] *Department of Materials Science and Engineering, Cornell University, Ithaca, NY*
[4)] *Present address: Center for Soft Matter Research, Department of Physics, New York University, New York, NY*
[5)] *To whom correspondence should be addressed: jd732@cornell.edu*
[6)] *To whom correspondence should be addressed: et106@wellesley.edu*

S1. BOND ANGLE ANALYSIS

Our topological analysis of cluster structure (Section 3C, main text) measures the evolution of different ring types in the bond network of each cluster, as cluster size N increases, and does not measure how bond angles actually shift as N increases. In this section, we measure distributions of bond angles for different values of N in our four systems, to provide additional details regarding how cluster geometries shift with system size.

To calculate bond angles, we order the nearest-neighbor bonds of each particle in the system counterclockwise, and measure the angles between adjacent bonds. For every particle k, we evaluate the set of nearest-neighbor bond angles θ_{ij}, where particles i and j are nearest neighbors of k and

$$\theta_{ij} = \cos^{-1}\left(\frac{\vec{r}_{ik}\cdot\vec{r}_{jk}}{r_{ik}r_{jk}}\right),$$

where $\vec{r}_{ik} = \vec{r}_i - \vec{r}_k$ and $\vec{r}_i$ is the position of particle i. We note that we only evaluate adjacent neighbor pairs (i, j) when neighbors are ordered counterclockwise around each particle k.

Fig. S1 shows histograms of bond angles for all particles in each cluster as a function of cluster size. Bond angle distributions for cluster sizes ranging from $N = 4$ to $N = 100$, as well as the bond angle distribution for the "bulk" cluster at $N = 625$, are shown for each system. In all cases, clusters have bulk-like bond angle distributions at high values of N, near $N = 100$.

We next show bond angle histograms for bonds at two distinct length scales, corresponding to the "short" and "long" bonding length scales discussed in the main text, to further tease apart distinctions in cluster geometry as cluster size increases. Here, we define all bonds with distance $r < 1.3$ to be the short bonds associated with the first well in the pair potential for all systems (except square), and we define all bonds with distance $1.3 < r < r_{max}$ to be the long bonds associated with the second well in the pair potential for all systems (except square). We set r_{max} uniquely for each system in order to investigate specific bonding regimes. The pair potential for the honeycomb and square systems goes to zero at smaller r than the pair potential for the triangular and rhombic systems. Thus, for the honeycomb and square systems we set r_{max} to a smaller value in order to only investigate bonds that contribute to the potential energy of the cluster. For these systems, we set $r_{max} = 1.9$. For the triangular and rhombic systems we set r_{max} to higher values (2.3 and 2.5, respectively) in order to capture all bonds associated with the second well in each pair potential. For each system, we show distributions of "short" and "long" bonds at three different values of N (small, intermediate, and large), to demonstrate changes in bonding geometry as cluster size increases. We group our results into two figures: one which shows bond angle evolution for the honeycomb and square systems (Fig. S2), and one which shows bond angle evolution for the triangular and rhombic systems (Fig. S3).

We first discuss the honeycomb and square systems. In Fig. S2a (top panel), the distribution of bond angles for the honeycomb system at $N = 5$ shows that all bonds within the cluster have length $1.3 < r < 1.9$, and all bond angles are around 60, 120, and 180 degrees. Consistent with the observations in the main text, this distribution indicates that the cluster consists of close-packed particles at the bonding distance corresponding to the deeper minimum in the potential well. At $N = 20$ (Fig. S2a, middle panel) and $N = 80$ (Fig. S2a, bottom panel), the system's geometry is more complex, containing bonding at shorter distances

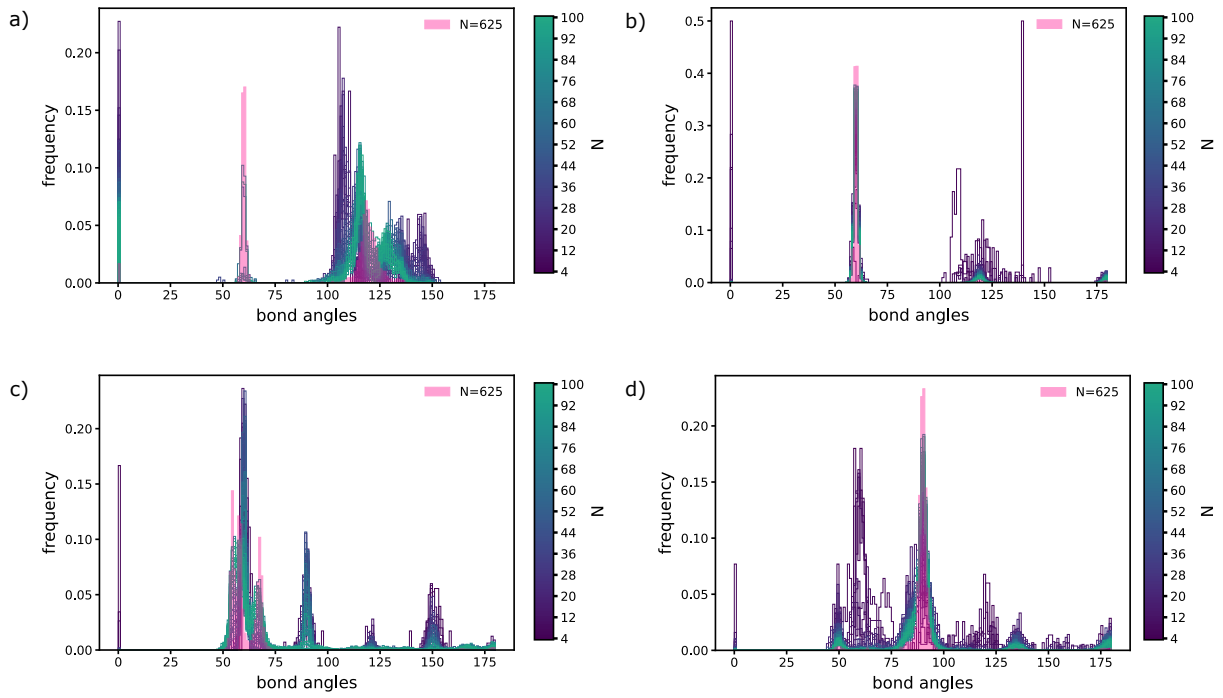

FIG. S1. **Bond angle distributions approach those of the bulk as cluster size N increases.** Panels show overlaid bond angle histograms for cluster sizes ranging from $N = 4$ (purple) to $N = 100$ (green), as well as the bond angle histogram for $N = 625$ (pink), for the (a) honeycomb, (b) triangular, (c) rhombic, and (d) square systems. In all cases, distributions are normalized such that they represent probability densities, to compare across system sizes. For $N = 4$ to $N = 100$, distributions are aggregated over 5 replicates each, and for $N = 625$, distributions are aggregated over 21 replicates each.

$r < 1.3$. These shorter bonds form angles that are distributed in two peaks near 125 degrees, showcasing that the clusters contain pentagonal and squashed hexagonal motifs formed from nearest neighbors at bond distances $r < 1.3$. At the larger values of N, the bond angles formed by the longer bonds are less useful for understanding structure. At $N = 20$ and $N = 80$, they form angles primarily around 30 and 60 degrees.

In Fig. S2b (top panel), the distribution of bond angles for the square system at $N = 6$ demonstrates that bonds are made up of short and long lengths. The cluster forms an irregular pentagon with one central particle; the bonds from the central particle to the surrounding pentagon of neighbors are short, and the bonds between adjacent neighbors in the pentagon are a mix of short and long. Thus the short bonds form smaller angles around 55 and 65 degrees, and the long bonds form larger angles around 110 degrees. Angle distributions are wide, indicating bonding flexibility. At $N = 12$ (Fig. S2b, middle panel), the bond angle distributions for both the short and long bonds are peaked around 90 degrees, indicating that the cluster now consists of particles bonded in square motifs. And at the larger system size $N = 80$ (Fig. S2b, bottom panel), all bond angle distributions are even more tightly peaked around 90 degrees, indicating more regularity in the square motifs in the cluster.

Bond angle distributions are especially useful for understanding distinctions between the triangular and rhombic systems as cluster size increases. At the smallest system sizes, each system forms distinct structures. The triangular system at $N = 5$ (Fig. S3a, top panel) primarily forms a pentagonal motif, where adjacent particles in the pentagon have short bonds ($r < 1.3$) between them, and non-adjacent particles have long bonds ($1.3 < r < 1.9$) between them. Bond angles between short bonds are thus primarily around 110 degrees, and bond angles between long bonds are primarily around 30 degrees. The rhombic system at $N = 6$ (Fig. S3b, top panel) primarily forms a subset of the snub square tiling consisting of a square motif with two adjacent equilateral triangles. Adjacent particles in the square and triangle motifs have short bonds between them, and non-adjacent particles have long bonds between them. Thus the short bonds have angles between them primarily of 60 and 90 degrees, and the long bonds have angles between them primarily of 30

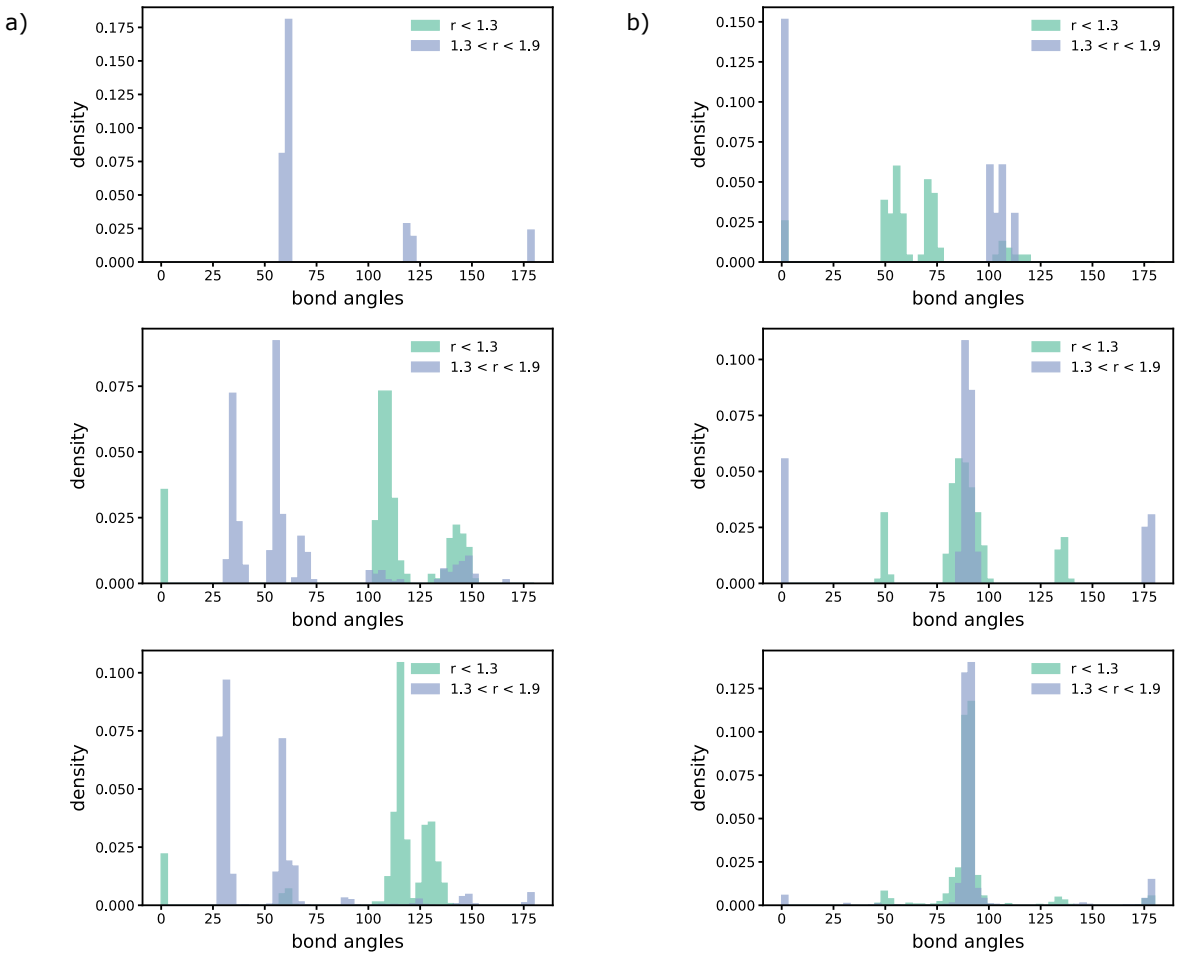

FIG. S2. **Select bond angle distributions for short and long bonds in the honeycomb and square systems at small, intermediate, and large values of N.** (a) Bond angle distributions for the honeycomb system are shown at $N = 5$ (top), $N = 20$ (middle), and $N = 80$ (bottom). (b) Bond angle distributions for the square system are shown at $N = 6$ (top), $N = 12$ (middle), and $N = 80$ (bottom). Short bonds, with lengths $r < 1.3$, are shown in green, and long bonds, with lengths $1.3 < r < 1.9$, are shown in blue. In all cases, distributions are normalized such that they represent probability densities, to compare across system sizes, and aggregated over 5 replicates each.

and 60 degrees. At intermediate system sizes, the triangular system showcases equilateral triangular motifs, with adjacent particles separated by short bonds, while the rhombic system showcases another subset of the snub square tiling consisting of square and triangle motifs (with adjacent particles separated by short bonds.) These differences in structure are reflected in the bond angle distributions. In the triangular system at $N = 10$ (Fig. S3a, middle panel), short bonds form angles primarily peaked around 60 and 120 degrees, while by contrast, in the rhombic system at $N = 20$ (Fig. S3b, middle panel), short bonds form angles primarily peaked around 60 and 90 degrees. The bond angle distributions corresponding to the long bonds are more complicated and less informative about structure at this system size.

At the largest system sizes, bond angle distributions reflect an important structural distinction between the triangular and rhombic systems. At $N = 80$, the triangular system (Fig. S3a, bottom panel) forms clusters that consist of the regular triangular lattice, with short bonds between adjacent particles in the lattice and long bonds between non-adjacent particles. By contrast, the rhombic system at $N = 80$ (Fig. S3b, bottom panel) forms clusters that consist of an irregular triangular lattice, with short bonds between adjacent particles in the lattice and long bonds between non-adjacent particles. In both systems, the long bonds form

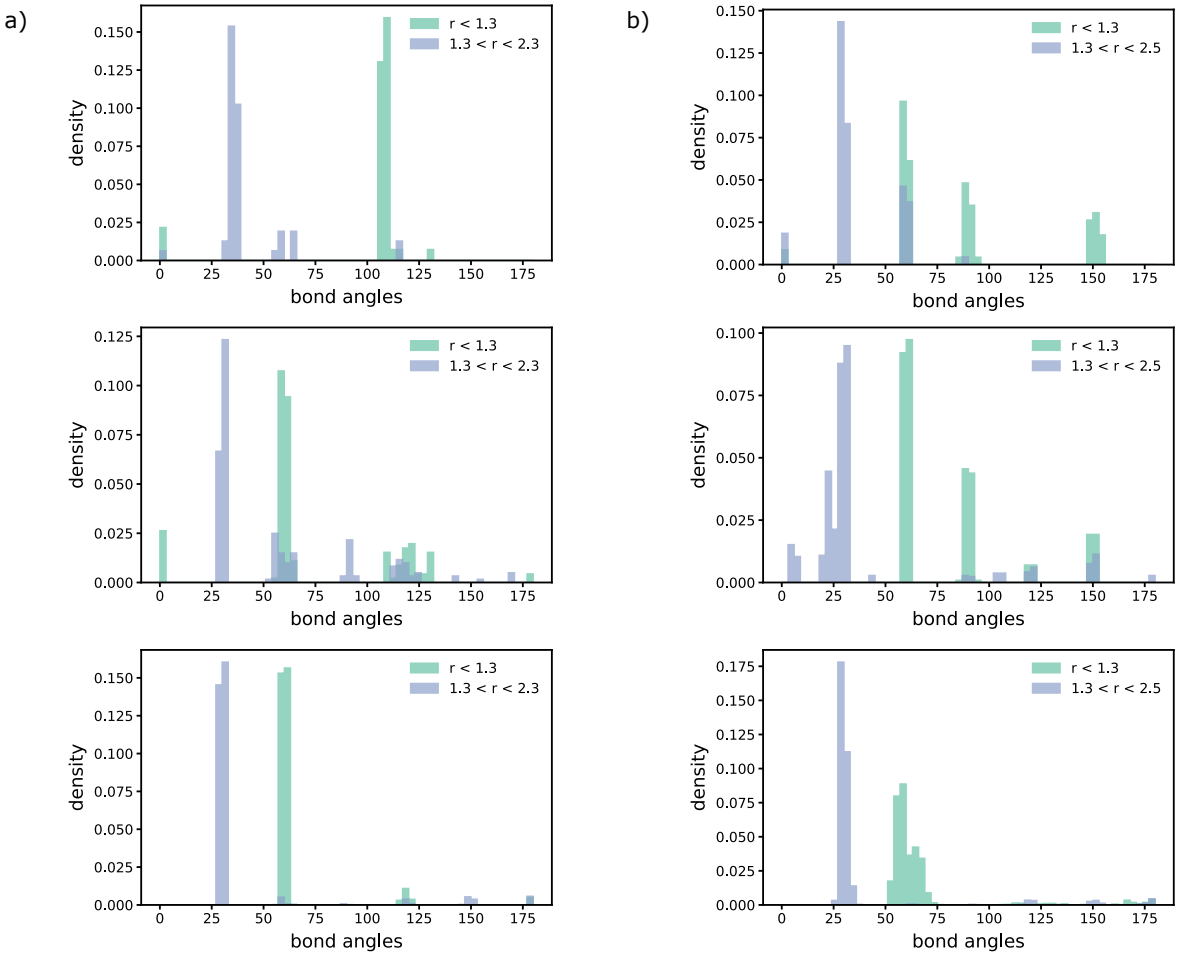

FIG. S3. **Select bond angle distributions for short and long bonds in the triangular and rhombic systems at small, intermediate, and large values of N.** (a) Bond angle distributions for the triangular system are shown at $N = 5$ (top), $N = 10$ (middle), and $N = 80$ (bottom). (b) Bond angle distributions for the rhombic system are shown at $N = 6$ (top), $N = 20$ (middle), and $N = 80$ (bottom). Short bonds, with lengths $r < 1.3$, are shown in green, and long bonds, with lengths $1.3 < r < 2.3$ and $1.3 < r < 2.5$, respectively, are shown in blue. In all cases, distributions are normalized such that they represent probability densities, to compare across system sizes, and aggregated over 5 replicates each.

angles that are tightly peaked around 30 degrees. Bond angle distributions for the short bonds, however, reflect a difference between regularity and irregularity: For the triangular system, short bond angles are sharply peaked around 60 degrees, while for the rhombic system, short bond angles are much more widely peaked around 60 degrees. In the rhombic system, the short bonds that form the triangles are at angles close to 60 degrees in an ordered pattern, but not exactly 60 degrees. (This can also be seen in the three sharp pink peaks in (Fig. S1c).

S2. BULK ENERGIES

In this section, we report the energies of the bulk clusters simulated at $N = 625$. Interestingly, we found through our analysis that two of the systems (honeycomb and rhombic) form predominant structures at this system size which seem to be at higher energy than competing crystalline polymorphs which occur at much lower frequency. Entropic or kinetic effects may therefore play a significant role in the stabilization of these

bulk structures.

For the honeycomb system, 19 out of the 21 replica simulations at $N = 625$ formed the honeycomb structure by visual inspection, each containing fewer than 10 defects in the form of inserted particles into the hexagonal "holes" in the honeycomb structure. The energy per particle for these replicas for all bonds is $\langle E(0, 2.5)/N\rangle = -3.212$, where the average is taken across all replicas, with standard deviation 0.004. Two of the 21 replica simulations contained more than 10 defects, meaning that a non-negligible portion of each cluster assumed the triangular structure. The energy per particle for these replicas for all bonds is $\langle E(0, 2.5)/N\rangle = -3.311$, where the average is taken across all replicas, with standard deviation 0.058. For the triangular system, 21 out of the 21 replica simulations at $N = 625$ formed the triangular structure by visual inspection, with some replicas containing defects in the form of missing particles creating hexagonal "holes" in the cluster. The energy per particle for all bonds is $\langle E(0, 2.5)/N\rangle = -5.539$, where the average is taken across all replicas, with standard deviation 0.009. For the rhombic system, 21 out of the 21 replica simulations at $N = 625$ formed the rhombic structure by visual inspection. The energy per particle for all bonds is $\langle E(0, 2.5)/N\rangle = -5.669$, where the average is taken across all replicas, with standard deviation 0.014. We note, however, that we observed the persistence of the snub square tiling in some replicas of large N clusters, always at lower energy than corresponding replicas which formed the rhombic structure. For example, at $N = 92$, two of the five replicas formed the snub square tiling, and had energy per particle equal to -5.02, approximately. By contrast, the three replicas at $N = 92$ which formed the rhombic structure had energy per particle ranging from -5.00 to approximately -4.99. For the square system, 21 out of the 21 replica simulations at $N = 625$ formed the square structure by visual inspection. The energy per particle for all bonds is $\langle E(0, 2.5)/N\rangle = -3.102$, where the average is taken across all replicas, with standard deviation 0.001.